Research Square

Preprints are preliminary reports that have not undergone peer review.
They should not be considered conclusive, used to inform clinical practice,
or referenced by the media as validated information.

Combined DCS–DRS Characterization of Cerebral Flow–Metabolic Responses in Behaviorally Defined Groups During Graded Isoflurane Exposure in Rats

Yoonho Oh
Gwangju Institute of Science and Technology
Myeongsu Seong
Xi'an Jiaotong-Liverpool University
Sungchul Kim
Gwangju Institute of Science and Technology
Seonghyun Kim
Gwangju Institute of Science and Technology
Jaeyoung Bae
Yonsei University College of Medicine
Jae Yoon Hwang
Daegu Gyeongbuk Institute of Science and Technology
Jae Gwan Kim
jaekim@gist.ac.kr

Gwangju Institute of Science and Technology

Research Article

Keywords: Anesthetic susceptibility, Cerebral blood flow, Cerebral metabolic rate of oxygen, Diffuse correlation spectroscopy, Diffuse reflectance spectroscopy, Isoflurane

Posted Date: October 7th, 2026

DOI: https://doi.org/10.21203/rs.3.rs-11137298/v1

License: This work is licensed under a Creative Commons Attribution 4.0 International License.
Read Full License

Additional Declarations: No competing interests reported.

Abstract

Background

Individual differences in anesthetic depth and recovery remain poorly understood. Near-infrared spectroscopy tracks cortical hemoglobin and oxygenation but not cerebral blood flow (CBF) or oxygen metabolism. We combined diffuse correlation spectroscopy (DCS) with diffuse reflectance spectroscopy (DRS) to measure relative CBF (rCBF), tissue oxygen saturation (StO_2), and hemoglobin concentration changes, and derive relative cerebral metabolic rate of oxygen ($rCMRO_2$) in the rat frontal cortex. Eight male Sprague-Dawley rats underwent 3.0% induction and stepwise 2.5–1.0% maintenance, with awake and recovery recordings. Animals were classified post hoc as 'not awake during anesthesia' (NAA, n = 4) or 'awake during anesthesia' (AA, n = 4) based on spontaneous movement with abrupt increases from the awake baseline in oxygenated hemoglobin (ΔOHb) and total hemoglobin (ΔTHb) concentrations at 1.0% isoflurane.

Results

During induction, peak rCBF was 346% versus 252% of the pre-induction awake value in AA versus NAA animals, and the maximum rate of increase was 11.9 versus 6.1 percentage points per second, respectively (p = 0.029 each). StO_2 and oxygenated (OHb), deoxygenated (RHb), and total (THb) hemoglobin concentrations showed no between-group difference in peak or maximum rate of increase. At 2.5%, rCBF was 168% in AA and 132% in NAA animals (p = 0.029). At 1.0%, rCBF was 297% versus 123% and $rCMRO_2$ was 117% versus 62%, based on a 60-s window centered on the movement-associated StO_2 peak in AA animals and the final 60 s in NAA animals (both p = 0.029). No between-group StO_2 or hemoglobin comparison was significant during maintenance. During recovery, the awake-baseline change in deoxygenated hemoglobin concentration (ΔRHb) was higher in NAA than in AA animals (p = 0.029). Emergence latency was 94 ± 42 s in AA animals and 580 ± 105 s in NAA animals (p = 0.029, absolute Hedges' g = 5.3).

Conclusions

AA animals showed greater rCBF responses than NAA animals during induction, at 2.5%, in the group-specific 1.0% windows, where $rCMRO_2$ was also higher. DCS revealed blood-flow differences not detected by DRS-based measures. These findings do not establish lower isoflurane sensitivity because grouping was post hoc and sensitivity was not measured directly.

Background

The cerebral response to general anesthesia is not uniform across individuals. In clinical and experimental settings alike, subjects exposed to similar anesthetic conditions can differ substantially in responsiveness[1], time to recovery[2], and the depth of suppression reached[3], yet the physiological basis of this variability is incompletely understood. Anesthetic agents alter cerebral blood flow (CBF) and cerebral metabolism in agent- and dose-dependent ways[4,5]. Isoflurane exerts a direct cerebral vasodilatory effect while depressing metabolic demand, so CBF and cerebral oxygen metabolism need not change in parallel[4,6,7]. Characterizing how CBF and cerebral oxygen metabolism change relative to one another may therefore help clarify physiological differences in anesthetic response.

Tissue oxygenation reflects the balance between oxygen delivery and oxygen consumption rather than either quantity on its own. If delivery and consumption change proportionally, tissue oxygenation may remain similar even when both processes differ markedly between individuals. These considerations raise the question of whether CBF and cerebral oxygen metabolism provide information about individual anesthetic responses that is not evident from tissue oxygenation or hemoglobin measures alone.

Optical neuromonitoring offers continuous, minimally invasive or noninvasive measurement of cortical hemodynamics during anesthesia. Near-infrared spectroscopy (NIRS) has been used to measure how oxygenated hemoglobin (OHb), deoxygenated hemoglobin (RHb), and total hemoglobin (THb) concentrations change with anesthetic depth. Electroencephalography (EEG) and EEG-derived indices such as the bispectral index (BIS) have been used to monitor anesthetic state[8–11]. A prior rat study combining NIRS and local field potential (LFP) recordings described graded hemoglobin and electrophysiological responses during graded isoflurane anesthesia[12]. Hemoglobin-based optical measurements, however, do not measure CBF directly and cannot by themselves estimate cerebral oxygen metabolism. EEG, BIS, and LFP provide complementary information about neural state, but likewise do not directly measure CBF.

Diffuse correlation spectroscopy (DCS) estimates a blood flow index (BFI) from temporal intensity fluctuations in light that has undergone multiple scattering in tissue[13,14]. When DCS and diffuse reflectance spectroscopy (DRS) are co-registered to sample overlapping cortical tissue, DCS-derived relative CBF (rCBF) and DRS-derived tissue oxygen saturation (StO_2) can be combined to derive a parameter relevant to cerebral oxygen metabolism, the relative cerebral metabolic rate of oxygen ($rCMRO_2$)[15–18]. Continuous co-measurement, therefore, allows changes in cerebral perfusion to be compared with changes in derived $rCMRO_2$ during anesthesia.

Previous optical studies showed that CBF and cerebral oxygen metabolism change during anesthesia, but their designs addressed different questions. In patients receiving propofol, rCBF and $rCMRO_2$ decreased during induction and increased during recovery, and the timing of these changes correlated with BIS[19]. Tagliabue et al. also found substantial variation among patients. Because propofol dosing and perioperative management were individualized, the patients were not compared during the same graded anesthetic exposure. The clinical study, therefore, could not determine how much of the variation

reflected individual cerebral responsiveness rather than differences in exposure or clinical context. In another study that used multi-parametric photoacoustic microscopy, CBF and $CMRO_2$ were measured in mice after equilibration at 0.5, 1.0, and 1.5 times the minimum alveolar concentration (MAC) of isoflurane[20]. Under normoxia, CBF was higher and $CMRO_2$ lower during anesthesia than during wakefulness, but $CMRO_2$ did not differ significantly among the three anesthetized levels. The photoacoustic microscopy study described stabilized responses at fixed isoflurane concentrations, and did not measure transient responses to concentration changes because measurements began after at least 15 min of equilibration, and each scan required approximately 15 min. More recently, a randomized trial continuously monitored relative StO_2 and $rCMRO_2$ during the first 30 min after positioning for shoulder surgery[21]. The 30-min averages did not show significant main effects of propofol versus sevoflurane or phenylephrine versus ephedrine. Temporal analysis nevertheless showed that relative StO_2 decreased and $rCMRO_2$ increased over time. Compared with ephedrine, phenylephrine was associated with a greater decline in relative StO_2 and a greater increase in $rCMRO_2$. The time-resolved analysis, therefore, detected changes during maintenance that were not apparent in the 30-min averages. The trial was designed to compare treatment strategies during surgery, not to isolate individual responses to a standardized graded anesthetic challenge.

Taken together, the clinical studies measured changes during induction, recovery, and maintenance, whereas the animal imaging study compared stabilized anesthetic levels. None of these studies combined continuous flow and metabolic monitoring with the same graded anesthetic sequence in every subject.

Meanwhile, Choi et al., our previous study, used a graded isoflurane protocol and observed two different responses at 1.0% isoflurane[12]. ‘Awake during anesthesia’ (AA) animals showed abrupt concentration increases from the awake baseline in oxygenated hemoglobin (ΔOHb) and total hemoglobin (ΔTHb), an awake-like LFP pattern without burst suppression, and spontaneous movement. ‘Not awake during anesthesia’ (NAA) animals retained burst suppression and showed neither spontaneous movement nor the abrupt ΔOHb and ΔTHb increases seen in AA animals. Thus, the study by Choi et al. linked the hemoglobin response to a difference in cortical electrical state under a common exposure. Because Choi et al. did not measure CBF or $CMRO_2$, the study could not determine whether the two groups also differed in cerebral perfusion and cerebral oxygen metabolism across the anesthetic course.

Here, we recorded DCS and DRS signals simultaneously over the frontal cortex of male Sprague-Dawley rats during a stepwise isoflurane protocol, with an awake baseline and a post-emergence recovery recording. Across the stage-wise epochs, we analyzed six hemodynamic and metabolic measures: DCS-derived rCBF; four DRS-derived measures (StO_2, ΔOHb, ΔRHb, ΔTHb); and $rCMRO_2$ derived from rCBF and StO_2. Animals that moved and showed abrupt increases in ΔOHb and ΔTHb during the 5-min stage at 1.0% isoflurane were classified as AA. Animals showing neither movement nor these hemoglobin increases during the same 5-min stage were classified as NAA. The stage-wise analyses compared all six hemodynamic and metabolic measures between groups. A separate induction-kinetics analysis

compared AA and NAA animals for the peaks and maximum rates of increase of rCBF, StO_2, OHb, RHb, and THb, each normalized to its separate pre-induction awake value. We examined whether group differences were already present during induction and the 2.5–1.5% maintenance stages, before the spontaneous movement and ΔOHb and ΔTHb increases used for classification at 1.0% isoflurane.

Methods

Animals

Eight male Sprague-Dawley rats (body weight 340–366 g; age 14–18 weeks) were used. Animals were housed at a constant room temperature (24 ± 1°C) with free access to food and water under a day–night cycle (lights on at 09:00 and off at 18:00). All procedures were approved by the Institutional Animal Care and Use Committee of the Gwangju Institute of Science and Technology (approval no. GIST-2019-060) and were carried out in accordance with the institution's animal care guidelines.

Surgical preparation and anesthesia protocol

Four custom-made fiber-based optodes were implanted over the frontal skull of each rat to collect signals from the prefrontal cortex, a region implicated in sleep and conscious visual perception[22,23] and previously examined during graded isoflurane anesthesia in rats[12]. For implantation, each rat was anesthetized with an intramuscular injection of a cocktail of ketamine hydrochloride (100 mg/kg) and xylazine (7 mg/kg) and fixed in a stereotaxic frame. The pericranium of the frontal area was removed, and the skull was exposed under 2.5% isoflurane delivered through a nasal cone. Four holes were drilled at 0.5 mm and 4 mm anterior to bregma and ± 1.75 mm lateral to the midline (Fig. 1(A)). One optode pair was used for DCS and the other for DRS. The pairs were arranged so that their probed cortical volumes overlapped at the prefrontal site. The optical ferrules of the optodes were fixed on the skull with dental cement (Fig. 1(B)) to suppress the influence of scalp and motion artifacts on cerebral hemodynamic signals. After surgery, each rat was treated with antiseptics and given at least four days for recovery before measurement.

Figure 1. Experimental design and optical setup. (A) Optode geometry on the rat skull (dorsal view, referenced to bregma/lambda): the four ferrules were placed bilaterally at 0.5 and 4.0 mm anterior to bregma and 1.75 mm lateral to the midline. The diagonal source–detector separation for each modality was approximately 5 mm, and the bilateral optodes within each anterior–posterior row were 3.5 mm apart. (B) Sagittal schematic of the implanted ferrules and fibers fixed to the skull with dental cement, coupling light into and out of the cortex. (C) Instrumentation: an 852-nm diffuse correlation spectroscopy (DCS) source and a broadband diffuse reflectance spectroscopy (DRS) source delivered light through separate fibers to the frontal cortex. Light collected by the DCS detector fiber passed through the wavelength division multiplexer (WDM) to the single-photon counting module and counter/timer, whereas diffusely reflected light collected by the DRS detector fiber was sent to the

spectrometer. Breathing gas mixed with isoflurane was delivered via a gas tube connected to a vaporizer/gas mixer, and body temperature was maintained with a heating pad. (D) Protocol timeline: 30-min awake baseline, anesthesia induction with 3.0% isoflurane in 50% oxygen and positioning, four stepwise maintenance stages (2.5, 2.0, 1.5, and 1.0% isoflurane in 50% oxygen; 2.5% isoflurane for 7 min, subsequent stages 5 min each), isoflurane discontinuation followed by observation until the first spontaneous movement, and a 30-min recovery recording.

The present study used an independent cohort and reproduced the anesthesia protocol used in the study by Choi et al.[12]. The skull-fixed optodes enabled continuous recording throughout the protocol. After a 30-min awake baseline was recorded from each freely moving rat, 3.0% isoflurane was delivered through the nasal cone in 50% oxygen, with nitrogen as the balance gas, for 3 min, following the protocol described previously. The isoflurane concentration was then lowered to 2.5% and maintained for 7 min. The first 2 min were used as a settling period after the concentration was reduced from 3.0% to 2.5%, following the previous protocol[12]. The concentration was then reduced by 0.5% every 5 min to a final concentration of 1.0%. Among the four maintenance stages, 2.5% was the deepest and 1.0% the lightest. Movement under anesthesia, used to assign the groups, was scored during the 1.0% stage. Following the 1.0% isoflurane stage, isoflurane was discontinued. Emergence latency was measured from discontinuation to the first spontaneous movement of any kind, including an eye blink, whisker movement, or whole-body movement. This first movement was used as the behavioral emergence endpoint. After the first spontaneous movement was observed, recording continued for 30 min before the rat was returned to its cage. The experimental design is summarized in Fig. 1(D). Respiration was monitored in real time with a gas analyzer (B40, GE Healthcare) via a customized low-dead-space nasal cone. A technical recording problem prevented the respiratory data from being archived for quantitative analysis. Body temperature was maintained with a heating pad during recording.

Behavioral group classification

For the post hoc classification, animals were classified as AA when spontaneous movement occurred together with abrupt increases in ΔOHb and ΔTHb while 1.0% isoflurane was still being delivered, consistent with the criteria described in our previous study[12]. Animals were classified as NAA when neither spontaneous movement nor abrupt increases in ΔOHb and ΔTHb occurred. The AA label is retained for continuity and denotes movement during maintained 1.0% isoflurane, not recovery of the righting reflex or complete emergence from anesthesia. Emergence latency was measured separately after isoflurane discontinuation as the time to the first spontaneous movement of any kind. Movement was scored in real time while the optical signals were being monitored. As in our previous study[12], spontaneous movement and the abrupt ΔOHb and ΔTHb increases occurred together in the present cohort, and final classification used the behavioral observation and concurrent optical traces jointly. Because the movement and hemoglobin increases at 1.0% isoflurane were used to classify the animals, between-group comparisons of the six hemodynamic and metabolic measures at 1.0% isoflurane characterize physiology during the classification period. Nevertheless, the hemodynamic signals at 1.0%

isoflurane do not establish whether AA and NAA animals could be distinguished independently of the classification period.

Optical instrumentation

Figure 1(C) shows the combined DCS–DRS system used to obtain DCS-derived rCBF and DRS-derived tissue oxygenation from overlapping sensitivity regions in the frontal cortex.

The DRS system includes a tungsten-halogen broadband light source (HL-2000-HP, Ocean Optics), a 16-bit charge-coupled device (CCD) spectrometer (USB4000, Ocean Optics), and two 400-μm-core multimode fibers (FT400EMT, Thorlabs). Each reflectance spectrum was normalized to its value at 500 nm, and the 620–800-nm region was analyzed. The spectra were fitted with steady-state diffuse-reflectance models[24,25] incorporating a vessel-packaging correction[26], hemoglobin extinction coefficients[27], wavelength-dependent reduced scattering[28], and blood-volume and oxygenation parameterizations used in diffuse optical spectroscopy[29,30]. The fitted blood-volume fraction and tissue oxygen saturation were used to derive OHb, RHb, and THb concentrations; ΔOHb, ΔRHb, and ΔTHb were then calculated as concentration changes from the awake baseline. The 620–800-nm fitting range excluded interference from the 852-nm DCS light source[30].

The DCS system includes an 852-nm continuous-wave laser (DL-852-100-SO, coherence length > 10 m, CrystaLaser), a single-photon counting module (SPCM-AQRH-12FC, Excelitas Technologies), and a wavelength-division multiplexer (RNN50HF, Thorlabs). Light was delivered to the tissue through a fiber attenuator with a 200-μm core (BB-100-11-685-200/240-QM-35-33-3-1-SP, OZ Optics), which also set the incident optical power, and the backscattered light was collected by a single-mode fiber (P1-780A-FC-2, Thorlabs) coupled to the single-photon counting module. Relative DCS-derived CBF changes have previously been validated against arterial spin labeling magnetic resonance imaging (ASL-MRI) in rats and against phase-encoded velocity mapping MRI measurements of cerebral venous outflow in pediatric patients[31,32]. The measured normalized intensity autocorrelation function, $g_2(\tau)$, where τ is correlation delay time, was fitted using the semi-infinite the Green's function solution of the correlation-diffusion Eq. 1[4] together with the Siegert relation[33]. The coherence factor, β, and BFI ($=\alpha D_B$), where α is the fraction of dynamically scattering particles and D_B is the effective Brownian diffusion coefficient, were estimated simultaneously by nonlinear least-squares fitting[34]. Fixed optical properties at 852 nm were the absorption coefficient ($\mu_a = 0.0334\ \mathrm{mm^{-1}}$) and reduced scattering coefficient ($\mu'_s = 1.330\ \mathrm{mm^{-1}}$), calculated using the wavelength-dependent tissue optical-property framework described by Jacques[28]. rCBF was calculated by normalizing BFI to the corresponding awake-baseline BFI for each animal. The two sampling rates were set independently. For each system, the detected intensity was adjusted to provide an adequate signal without detector saturation, and the acquisition rate was set to the highest value that maintained this signal quality. The resulting rates were 3 Hz for the DRS spectrometer, limited by the integration time required for an adequate spectral signal-to-noise ratio, and 2 Hz for the DCS module, limited by the averaging time required for a stable

autocorrelation function. They were still sufficient to resolve the stage-wise changes analyzed here, which occurred over minutes. Each system was controlled by an in-house LabVIEW program (LabVIEW 2012, National Instruments), and data was processed in MATLAB (MATLAB R2013b, MathWorks). Further instrument details are given in our previous report[12,34].

Derived measures

Across the stage-wise epochs, the six analyzed hemodynamic and metabolic measures were DCS-derived rCBF, DRS-derived StO_2 and hemoglobin concentration changes (ΔOHb, ΔRHb, and ΔTHb), and $rCMRO_2$ derived from rCBF and StO_2. $rCMRO_2$ was estimated using the relationship reported for rodent cortex, $\mathrm{rCMRO_2} = \mathrm{rCBF} \times (1 - \mathrm{StO_2}) \,/\, (1 - \mathrm{StO_{2,awake}})$[16], where $\mathrm{StO_{2,awake}}$ is the awake-baseline StO_2. StO_2 values were entered in the equation as fractions from 0 to 1. Because DRS and DCS were sampled at different rates, the StO_2 and rCBF time series were interpolated to 10 Hz before $rCMRO_2$ was calculated[35–37]. rCBF and $rCMRO_2$ were normalized to each animal's awake-baseline value, defined as 100%. ΔOHb, ΔRHb, and ΔTHb were reported as concentration changes from the awake baseline in μM, whereas StO_2 was reported as an absolute saturation percentage. For the separate induction-kinetics analysis, rCBF, StO_2, and the fitted OHb, RHb, and THb concentrations were normalized to their respective separate pre-induction awake values (100%) before peaks and maximum rates of increase were calculated. The anesthetic protocol stages and the optical acquisition and model parameters are summarized in Additional file 1: Table S7. The models and calculations used to derive these measures are described in Additional file 1, Supplementary Methods section 3.

Statistical analysis

Group values at each epoch were summarized as mean ± standard deviation (SD). Awake and recovery values were computed as medians over 120-s windows meeting signal-stability criteria (StO_2 coefficient of variation (CV) < 6% and THb CV < 8%). For the awake reference, one 120-s window was defined by working backward from the end of the awake period and then checked against these stability thresholds; the analysis did not search among multiple eligible windows or choose the interval according to the AA–NAA result. For the 2.5%, 2.0%, and 1.5% isoflurane stages, each animal's value for every hemodynamic and metabolic measure was calculated as the median over the final 60 s of the stage. For AA animals at 1.0% isoflurane, the median values of all six hemodynamic and metabolic measures were calculated using data from the same 60-s interval centered on each animal's StO_2 peak (peak ± 30 s), preserving their relative temporal alignment. Thus, the 1.0% between-group comparison used a peak-centered 60-s interval in AA animals and the final 60 s of the stage in NAA animals. Because only the AA window was centered on the StO_2 peak, the 1.0% between-group comparison contrasted a movement-associated AA interval with the NAA end-of-stage interval. Thus, the two groups were compared using differently positioned 60-s windows, which are a peak-centered window for AA animals and the final 60 s of the stage for NAA animals. Meanwhile, the analyses of the hemodynamic signals from induction and 2.5%

isoflurane stages were performed before the spontaneous movement and abrupt increases in ΔOHb and ΔTHb used for classification, and did not use the group-specific 1.0% extraction windows.

Given the group size (n = 4 per group), the exact Mann–Whitney U test[38] was used for between-group comparisons, and effect-size magnitudes were reported as absolute Hedges' g ($|g|$)[39]. Dose-dependent trends were assessed with Page's trend test[40] and the Friedman test[41] across all four maintenance stages in NAA animals. For the AA animals, the StO_2-centered 1.0% window was excluded from the Page and Friedman tests because it sampled the movement-associated peak, whereas the hemodynamic parameters in 2.5%, 2.0%, and 1.5% isoflurane stages were taken from the final 60 s of each stage. Therefore, the Page and Friedman tests for AA animals were only performed for the 2.5%, 2.0%, and 1.5% stages. For Page's trend test, the reported two-sided p-value was twice the smaller of the two exact directional p-values, capped at 1. Because the study was exploratory, p-values were not adjusted for multiple comparisons. Several of the six hemodynamic and metabolic measures were related. Specifically, ΔOHb, ΔRHb, ΔTHb, and StO_2 were obtained from the same DRS measurements, and $rCMRO_2$ was derived from rCBF and StO_2. Findings across these related measures were therefore not treated as independent replications. Accordingly, each p-value was interpreted descriptively together with the corresponding effect size and per-animal values.

Within each group, consecutive plotted analysis epochs, including awake to 2.5% isoflurane, each adjacent pair of maintenance concentrations, and 1.0% isoflurane to recovery, were compared using two-sided paired tests. For each comparison, normality of the within-animal paired differences was assessed using the Shapiro–Wilk test. A paired t-test was used when normality was not rejected ($p > 0.05$), and an exact Wilcoxon signed-rank test was used otherwise. Within each group, each of the four maintenance stages and the recovery epoch shown in Fig. 2 was compared with the awake baseline using a two-sided paired t-test. The comparisons of each maintenance stage and recovery with the awake baseline are marked by asterisks in Fig. 2. To determine whether awake-baseline window length affected the stage-wise results in Table 1, the 2.5% and 1.0% between-group comparisons were repeated using awake windows of 60, 120, 180, 240, and 300 s. The induction analyses were not included because they used a separate pre-induction baseline. Statistical analysis was performed in Python using SciPy.

Use of generative artificial intelligence (AI)-assisted technologies

During manuscript preparation, the authors used Claude (Anthropic) and ChatGPT (OpenAI) to revise language, reorganize author-written text, and assist with formatting supplementary tables and figures derived from the authors' data. No AI tool was used to generate experimental data. All AI-assisted text and materials, including numerical values and interpretations, were reviewed and verified by the authors, who take full responsibility for the final content.

Figure 2. Relative cerebral blood flow (rCBF), tissue oxygen saturation (StO_2), concentration changes from the awake baseline in oxygenated hemoglobin (ΔOHb), deoxygenated hemoglobin (ΔRHb), and

total hemoglobin (ΔTHb), and derived relative cerebral metabolic rate of oxygen ($rCMRO_2$) during the awake baseline, isoflurane maintenance, and recovery periods in 'not awake during anesthesia' (NAA) and 'awake during anesthesia' (AA) animals. The left and right columns show the NAA and AA groups, respectively. Box plots show the awake baseline, four maintenance concentrations (2.5, 2.0, 1.5, and 1.0% isoflurane), and recovery, with per-animal values connected across periods. Awake and recovery values were calculated over 120-s windows. Maintenance values were calculated from the final 60 s of each stage, except for the AA values at 1.0%, which were calculated over 60-s windows centered on each animal's StO_2 peak. The Page and Friedman tests included all four maintenance concentrations in NAA animals and the 2.5, 2.0, and 1.5% concentrations in AA animals. The plotted AA values at 1.0% were excluded from the Page and Friedman tests. P_{trend}, Page's trend-test p; Friedman, Friedman-test p; ns, not significant. *: $p < 0.05$, **: $p < 0.01$, and ***: $p < 0.001$ for two-sided paired t-tests against the awake baseline ($n = 4$ per group). Source data are provided in Additional file 2.

Results

Stage-wise hemodynamic and metabolic responses during graded isoflurane anesthesia

Figure 2 shows all six hemodynamic and metabolic measures (rCBF, StO_2, ΔOHb, ΔRHb, ΔTHb, and $rCMRO_2$) in both groups across six stage-wise epochs: the awake baseline, maintenance at 2.5, 2.0, 1.5, and 1.0% isoflurane, and recovery. The 3.0% isoflurane anesthesia induction transient was analyzed separately (Fig. 3). The corresponding within-group trend statistics are tabulated in Additional file 1: Table S1. Stage-wise values, paired comparisons between consecutive plotted analysis epochs, and awake-baseline-window sensitivity results are provided in Additional file 1: Tables S2, S3, and S4, respectively.

In NAA animals ($n = 4$), ΔOHb, ΔTHb, and StO_2 decreased monotonically as isoflurane was reduced from 2.5 to 1.0% (Page's trend test $p < 0.001$ for each variable). Friedman tests also detected stage-dependent variation in ΔOHb, ΔTHb, and StO_2 (Additional file 1: Table S1). ΔRHb showed a significant ordered increase toward the awake baseline as isoflurane was reduced (Page's trend test $p = 0.008$). Mean StO_2 increased from 57.6 ± 12.9% during the awake baseline to 83.0 ± 7.1% at 2.5% isoflurane and then decreased to 78.6 ± 9.7% at 1.0% isoflurane, before returning to 57.4 ± 14.0% during recovery. Mean ΔOHb decreased from + 6.3 ± 2.6 μM at 2.5% isoflurane to + 4.6 ± 2.7 μM at 1.0% isoflurane, and mean ΔTHb decreased from + 3.7 ± 2.9 μM to + 2.4 ± 2.3 μM. Mean ΔRHb remained below the awake baseline at both 2.5% isoflurane (− 2.5 ± 0.9 μM) and 1.0% isoflurane (− 2.2 ± 0.8 μM). Mean $rCMRO_2$ remained below the awake-baseline value throughout anesthesia maintenance and increased monotonically from 53.0 ± 18.3% at 2.5% isoflurane to 62.4 ± 26.0% at 1.0% isoflurane (Page's trend test $p = 0.001$). Mean rCBF did not show a significant monotonic trend as isoflurane was reduced ($p = 0.101$): it was 132.4 ± 23.0% at 2.5% isoflurane, 136.4 ± 24.1% at 2.0% isoflurane, and 123.4 ± 27.5% at 1.0% isoflurane.

Although the highest mean rCBF occurred at 2.0% isoflurane, rCBF did not differ significantly between 2.5 and 2.0% isoflurane (paired t-test $p = 0.317$).

During recovery, mean ΔRHb was 0.6 ± 0.3 μM in NAA animals and − 0.5 ± 0.9 μM in AA animals (exact Mann–Whitney U test $p = 0.029$, $|g| = 1.32$). During recovery, rCBF, StO_2, ΔOHb, ΔTHb, and $rCMRO_2$ did not differ significantly between groups (all $p \geq 0.114$).

AA animals had a higher rCBF peak and maximum rate of increase during induction

During 3.0% induction, AA animals had a higher peak rCBF and a greater maximum rate of rCBF increase than those of NAA animals (Fig. 3, with per-animal values in Additional file 1: Table S5). Peak rCBF reached 346.0 ± 20.2% of the separate pre-induction awake value in AA animals and 251.5 ± 33.1% in NAA animals (Mann–Whitney U test, $p = 0.029$). Based on the unrounded group means, the AA peak was 38% higher (e.g., [(AA − NAA) / NAA] × 100%) than the NAA peak. The maximum rate of increase in rCBF normalized to the separate pre-induction awake value was 11.9 ± 3.8 percentage points per second in AA animals and 6.1 ± 1.3 percentage points per second in NAA animals ($p = 0.029$). Based on the unrounded group means, the AA rate was 94% higher than the NAA rate. We then checked whether AA and NAA animals also differed in the induction peak or maximum rate of increase of StO_2, OHb, RHb, or THb. Each induction measure was expressed as a percentage of its own separate pre-induction awake value, defined as 100%. For StO_2, OHb, RHb, and THb, neither the induction peak nor the maximum rate of increase differed significantly between AA and NAA animals. All p-values were at least 0.057 (Additional file 1: Table S8). Thus, rCBF was the only hemodynamic measure with a significant AA–NAA difference in the induction peak and the maximum rate of increase.

rCBF was higher in AA animals at 2.5% isoflurane

Mean rCBF was higher in AA than in NAA animals at each of the three maintenance concentrations that preceded the group-defining 1.0% isoflurane stage. At 2.5% isoflurane, mean rCBF was significantly higher in AA animals than in NAA animals (168.3 ± 11.5% vs 132.4 ± 23.0%; Mann–Whitney U test $p = 0.029$). At the same concentration, StO_2 did not differ significantly between AA and NAA animals (85.4 ± 0.8% vs 83.0 ± 7.1%; $p = 1.0$; Fig. 4). Meanwhile, mean $rCMRO_2$ at 2.5% isoflurane was 66.3 ± 1.4% in AA animals and 53.0 ± 18.3% in NAA animals, but the AA–NAA comparison was not significant ($p = 0.343$). At 2.0% isoflurane, mean rCBF was 164.5 ± 8.8% in AA animals and 136.4 ± 24.1% in NAA animals ($|g| = 1.35$). At 1.5% isoflurane, mean rCBF was 161.3 ± 7.0% in AA animals and 131.6 ± 25.9% in NAA animals ($|g| = 1.36$). The rCBF comparisons did not reach statistical significance at either 2.0% (exact Mann–Whitney $p = 0.057$) or 1.5% isoflurane ($p = 0.057$).

A transient increase in rCBF and $rCMRO_2$ accompanies spontaneous movement in AA animals at 1.0% isoflurane

Figure 5 shows rCBF, $rCMRO_2$, and StO_2 at 1.0% isoflurane. In AA animals, mean rCBF decreased modestly from 168.3% at 2.5% isoflurane to 164.5% at 2.0% and 161.3% at 1.5%. Over the same concentrations, mean StO_2 decreased from 85.4 ± 0.8% to 82.3 ± 1.4%, whereas mean $rCMRO_2$ increased from 66.3 ± 1.4% to 77.0 ± 3.8% but remained below the awake-baseline value. Over the same concentrations, mean ΔOHb and ΔTHb decreased from 4.6 ± 0.5 to 3.6 ± 0.6 μM and from 2.5 ± 1.1 to 1.9 ± 1.3 μM, respectively, while mean ΔRHb moved toward the awake baseline from − 2.0 ± 0.8 to − 1.7 ± 0.7 μM. These directions were consistent with those reported previously using the same graded isoflurane protocol[12]. At 1.0% isoflurane, every AA animal showed a brief StO_2 peak around spontaneous movement. Because this peak did not persist throughout the 1.0% stage, the 60-s analysis window was centered on each animal's peak. Within these peak-centered windows, mean rCBF reached 297.3 ± 35.3% and mean $rCMRO_2$ reached 117.4 ± 14.2% of the awake-baseline value. $rCMRO_2$ exceeded the awake-baseline value in all four AA animals (115, 103, 114, and 137%; Additional file 1: Fig. S1).

NAA animals did not show as significant changes in the hemodynamic measures as AA animals at 1.0% isoflurane when values from the AA peak-centered windows were compared with values from the final 60 s in NAA animals. rCBF was significantly higher (297.3 ± 35.3% vs 123.4 ± 27.5%, $p = 0.029$), and $rCMRO_2$ was also significantly higher (117.4 ± 14.2% vs 62.4 ± 26.0%, $p = 0.029$) in AA animals than NAA animals. The change in StO_2 from the awake baseline did not differ significantly between groups (22.5 ± 1.6 percentage points vs 21.0 ± 5.6 percentage points, $p = 0.486$). For rCBF and $rCMRO_2$, each animal's analysis-window value was expressed as a percentage of its awake-baseline value: (analysis-window value / awake-baseline value) × 100. StO_2 change was calculated for each animal as the analysis-window saturation minus the awake-baseline saturation and was reported in percentage points. Values are group means ± SD of the resulting per-animal values.

The AA values at 1.0% isoflurane were excluded from the Page and Friedman tests because the StO_2-centered window sampled the movement-associated peak, whereas the values at 2.5%, 2.0%, and 1.5% isoflurane were taken from the final 60 s of each stage. As a result, the tests for AA animals included only the 2.5%, 2.0%, and 1.5% isoflurane stages. Across these three stages, rCBF showed neither a significant ordered trend (Page's trend test $p = 0.218$) nor a significant overall stage effect (Friedman test $p = 0.368$). In contrast, Page's trend test showed a significant ordered trend for each of ΔOHb, ΔRHb, StO_2, and $rCMRO_2$ (all $p = 0.002$), as well as for ΔTHb ($p = 0.014$).

The same 60-s interval centered on each animal's StO_2 maximum was applied to rCBF, StO_2, ΔOHb, ΔRHb, ΔTHb, and $rCMRO_2$ so that all six hemodynamic and metabolic measures were evaluated during the same physiological period (Additional file 1: Fig. S3). Mean StO_2 within the four individual AA windows ranged from 84.0 to 86.4%.

At the 0.5-s temporal resolution of the DCS data, no consistent lead–lag between the rCBF and StO_2 increases could be resolved (Additional file 1: Fig. S2).

Table 1 summarizes all statistically significant between-group comparisons during induction, isoflurane maintenance, and recovery, together with selected nonsignificant comparisons.

Table 1
Comparison between the 'not awake during anesthesia' (NAA) and 'awake during anesthesia' (AA) groups

Measure and analysis stage	NAA (mean ± SD)	AA (mean ± SD)	*p* (Mann–Whitney)	|*g*|
Measures with a statistically significant AA–NAA difference				
rCBF at 2.5% (deep maintenance)	132.4 ± 23.0	168.3 ± 11.5	0.029	1.72
rCBF at 1.0%†	123.4 ± 27.5	297.3 ± 35.3	0.029	4.78
$rCMRO_2$ at 1.0%†	62.4 ± 26.0	117.4 ± 14.2	0.029	2.28
Induction rCBF peak (% of separate pre-induction awake rCBF)	251.5 ± 33.1	346.0 ± 20.2	0.029	3.00
Induction rCBF maximum rate of increase (percentage points per second)	6.1 ± 1.3	11.9 ± 3.8	0.029	1.75
ΔRHb during recovery (μM)	0.6 ± 0.3	−0.5 ± 0.9	0.029	1.32
Measures without a statistically significant AA–NAA difference				
$rCMRO_2$ at 2.5% (deep maintenance)	53.0 ± 18.3	66.3 ± 1.4	0.343	0.89
Change in StO_2 from the awake baseline at 1.0%†	+ 21.0 ± 5.6	+ 22.5 ± 1.6	0.486	0.30
ΔOHb at 1.0%† (μM)	4.6 ± 2.7	5.0 ± 0.8	0.486	0.20
ΔRHb at 1.0%† (μM)	−2.2 ± 0.8	−1.9 ± 0.8	0.686	0.25
ΔTHb at 1.0%† (μM)	2.4 ± 2.3	3.1 ± 1.6	0.886	0.30

Values are mean ± SD. Between-group *p*-values are from two-sided exact Mann–Whitney U tests ($n = 4$ per group). Bias-corrected effect-size magnitudes are reported as absolute Hedges' *g* (|*g*|), and the group means show the direction of each difference. Measures are grouped by whether a statistically significant AA–NAA difference was observed. Stage-wise rCBF and $rCMRO_2$ are expressed relative to each animal's awake-baseline value (awake = 100%); induction rCBF is expressed relative to the separate pre-induction awake value. The StO_2 change is reported in percentage points. ΔOHb, ΔRHb, and ΔTHb are reported as concentration changes from the awake baseline in μM. †For every 1.0% row, the AA value was calculated over the 60-s interval centered on each animal's StO_2 peak, whereas the NAA value was calculated over the final 60 s of the 1.0% stage.

The 2.5% and 1.0% comparisons listed in Table 1 were repeated using awake-baseline windows of 60, 120, 180, 240, and 300 s (Additional file 1: Table S4). Changing the awake-baseline window did not change the direction of any AA–NAA mean difference, and |*g*| values remained similar. The rCBF and $rCMRO_2$ differences at 1.0% isoflurane remained significant for every tested baseline window ($p = 0.029$). Every comparison that was nonsignificant with the 120-s window remained nonsignificant. At 2.5% isoflurane, rCBF remained higher in AA than in NAA animals for every baseline-window length, with |*g*| values of 1.2–1.9. The comparison yielded $p < 0.05$ only with the prespecified 120-s window ($p = 0.029$, compared with $p = 0.057–0.114$ for the other windows).

Emergence latency after isoflurane withdrawal

Emergence latency was markedly shorter in AA animals than in NAA animals (94 ± 42 s vs 580 ± 105 s, $p = 0.029$, $|g| = 5.3$), as shown in Fig. 6. Per-animal values are provided in Additional file 1: Table S6.

Discussions

Flow and metabolic differences between the behavioral response groups

Combined DCS–DRS identified between-group differences primarily in rCBF. AA animals had a higher rCBF peak and a higher maximum rate of rCBF increase during induction and higher rCBF than NAA animals at 2.5% isoflurane. At 1.0% isoflurane, rCBF was higher in the AA peak-centered windows than in the NAA end-of-stage windows. Among the maintenance-stage comparisons, a between-group difference in $rCMRO_2$ was detected only in the group-specific 1.0% windows. StO_2 and the hemoglobin concentrations did not differ significantly between groups during induction or isoflurane maintenance. During recovery, ΔRHb was higher in NAA than in AA animals, whereas rCBF, StO_2, ΔOHb, ΔTHb, and $rCMRO_2$ did not differ significantly.

StO_2 and rCBF describe different aspects of cerebral oxygen physiology. StO_2 indicates the fraction of hemoglobin that is oxygenated in the sampled tissue, whereas rCBF indicates blood delivery per unit time. Higher rCBF increases oxygen delivery, but its effect on StO_2 depends on how much of the delivered oxygen is extracted and consumed by the tissue[16,18]. If oxygen delivery and oxygen consumption increase together, StO_2 may change little even when rCBF increases substantially. Therefore, similar StO_2 values do not always imply similar blood flow. At 1.0% isoflurane, AA animals had higher rCBF than NAA animals, while StO_2 did not differ significantly. Because $rCMRO_2$ was calculated by combining rCBF with an oxygen-extraction term based on StO_2[16], the higher rCBF contributed directly to the higher $rCMRO_2$ in AA animals. Combined DCS–DRS therefore distinguished the between-group blood-flow difference that was not apparent from DRS-derived StO_2 or hemoglobin measures alone.

The rCBF differences during induction and at 2.5% isoflurane were observed before the movement and abrupt ΔOHb and ΔTHb increases used to define the groups at 1.0%. Thus, AA and NAA animals showed different CBF responses during earlier parts of the same anesthetic protocol. During induction, rCBF was the only hemodynamic parameter for which both the peak and the maximum rate of increase differed significantly between groups in this study. Also, rCBF was the only stage-wise hemodynamic measure that differed significantly between groups at 2.5% isoflurane. These findings identify different rCBF responsiveness between the groups but do not establish the underlying physiological mechanism. Thus, the 2.5% finding should be interpreted cautiously because statistical significance was observed only with the prespecified 120-s awake-baseline window (Additional file 1: Table S4). Future studies combining optical monitoring with arterial pressure and arterial blood-gas measurements, electrophysiological recordings, and controlled cerebrovascular-reactivity testing will be needed to determine whether the group difference reflects systemic hemodynamic effects, cerebrovascular responsiveness, or differences in neural activity.

Flow and metabolic changes during the 1.0% behavioral response

At 1.0% isoflurane, the higher rCBF and $rCMRO_2$ in AA animals were measured during the transient surrounding spontaneous movement. $rCMRO_2$ exceeded the awake baseline during the AA transient. This transient value is not directly comparable with the reductions after equilibration at fixed isoflurane concentrations reported in the photoacoustic microscopy study[20] because that study characterized stabilized responses rather than changes during movement or a concentration transition.

Choi et al. combined frontal-cortical NIRS and LFP recordings during the same stepwise isoflurane protocol[12]. At 1.0% isoflurane, AA animals showed abrupt increases in ΔOHb and ΔTHb, and their LFP no longer showed burst suppression and resembled the awake pattern. The concurrent hemoglobin and LFP changes indicated that the 1.0% response involved both cerebral oxygenation and cortical electrical activity, but the study did not measure the accompanying blood flow or oxygen metabolism. In the present AA animals, group-mean rCBF and estimated $rCMRO_2$ were above the awake baseline during the movement-associated hemoglobin response at 1.0% isoflurane. Thus, the two studies characterized different aspects of the 1.0% response, with the earlier NIRS–LFP study recording concurrent hemoglobin and cortical electrical changes, whereas the present DCS–DRS study measured rCBF and provided an optical estimate of $rCMRO_2$. However, because neuronal activity was not recorded in the present cohort, the relationship of these hemodynamic and metabolic changes to neuronal activity, including whether neurovascular coupling changed during the 1.0% response, could not be determined[12,42–45]. Addressing this question would require concurrent recording of LFP, or another measure of neuronal activity, alongside simultaneous measurements of DCS and DRS signals.

Because movement and abrupt ΔOHb and ΔTHb increases at 1.0% isoflurane defined the AA group, the concurrent rCBF and $rCMRO_2$ differences describe the movement-associated 1.0% response rather than an independent basis for group assignment. The abrupt ΔOHb and ΔTHb increases used for

classification describe how each animal's signals changed over time, whereas the between-group hemoglobin tests compared the median values from each animal's 60-s analysis window. These are different comparisons, so the absence of a significant between-group hemoglobin difference does not conflict with the use of the abrupt increases for classification.

Possible explanations for higher rCBF at 2.5% isoflurane

At 2.5% isoflurane, rCBF was higher in AA than in NAA animals, whereas StO_2 and $rCMRO_2$ did not differ significantly. Isoflurane alters CBF through cerebrovascular effects, including direct vasodilation and impaired autoregulation at higher concentrations, and through concurrent metabolic suppression[4–7,46–55]. Differences in vascular responsiveness, metabolic suppression, baseline physiology, or neural suppression[56–59] could therefore contribute to the higher rCBF in AA animals. The present data cannot distinguish among these possibilities because arterial pressure was not recorded, respiratory-gas records were unavailable for analysis, and neural activity and inspired and expired isoflurane concentrations were not measured. Future studies combining DCS and DRS with EEG or LFP, along with continuous monitoring of arterial pressure, respiratory gas, and anesthetic concentration, could further clarify the physiological basis of this group difference.

Emergence latency and possible state-transition differences

Group assignment incorporated spontaneous movement during maintained 1.0% isoflurane, whereas emergence latency measured the time to the first spontaneous movement after isoflurane was discontinued. Therefore, the shorter latency means that AA animals showed spontaneous movement sooner than NAA animals after isoflurane was discontinued. Post-discontinuation emergence latency does not independently validate the group classification because group assignment and emergence latency both depend on spontaneous movement.

AA animals had a higher induction rCBF peak and maximum rate of increase, higher rCBF at 2.5% isoflurane, and shorter post-discontinuation emergence latency than NAA animals. These findings show that the groups had different cerebral hemodynamic and behavioral responses at several parts of the same graded isoflurane protocol, but they do not imply that higher rCBF caused earlier movement.

Individual variation in neural inertia, defined as path-dependent resistance to transitions between responsive and unresponsive states, could have contributed to the between-group difference in emergence latency[60–62]. The present study cannot evaluate this possibility because responsiveness was not measured at matched anesthetic concentrations during induction and emergence, and neuronal activity was not recorded. Hence, the findings should not be interpreted as evidence of neural inertia. Future studies using bidirectional isoflurane steps with concurrent behavioral, EEG or LFP, and DCS–DRS measurements could test this possibility.

Study limitations

In addition to the limitations mentioned in the above sub-section, there are additional limitations that should be mentioned. 1) The animal study only involved a small cohort and was restricted to male rats. A future study may need to involve a larger population and both male and female animals to generalize the results. 2) The reported effect sizes and per-animal values were used to characterize the magnitude of the observed differences and to assess their consistency across animals within the present cohort. However, these within-cohort analyses do not constitute independent replication, and the findings require confirmation in a larger independent cohort. 3) Because rCBF and $rCMRO_2$ were normalized to each animal's awake baseline, the study cannot determine whether the groups differed in absolute awake CBF or $CMRO_2$. More advanced systems capable of estimating absolute hemodynamic parameters may be considered in a future study[35,36]. 4) Respiration was monitored during the experiments, but the respiratory gas records were not archived because of a technical recording problem. Also, arterial pressure was not recorded. Consequently, explanations involving arterial pressure or CO_2 tension could not be evaluated. 5) The DCS–DRS measurements sampled a localized volume of the frontal cortex, so the study cannot determine whether the between-group differences were also present in other brain regions or across the whole brain. 6) The 2-Hz DCS sampling rate could not resolve onset differences shorter than 0.5 s, so the temporal ordering of the rCBF and StO_2 increases remains unresolved. A higher sampling rate could be achieved in the future using detectors with higher sensitivity.

Conclusions

Combined DCS–DRS showed that AA and NAA animals differed in rCBF before and during the movement-associated response at 1.0% isoflurane. AA animals had a higher induction rCBF peak, a higher maximum rate of rCBF increase, and higher rCBF at 2.5% isoflurane than NAA animals. At 1.0% isoflurane, rCBF and $rCMRO_2$ were higher in the AA peak-centered windows than in the NAA end-of-stage windows. No statistically significant between-group differences were detected in StO_2 or the hemoglobin measures during induction or isoflurane maintenance. Thus, this study shows that DCS can be used to identify CBF differences that are not evident from DRS-based oxygenation or hemoglobin measurements. Given the post hoc group definition and four animals per group, the findings require replication in a larger independent cohort. The present findings do not establish rCBF or $rCMRO_2$ as markers of anesthetic susceptibility. Combined DCS–DRS may complement DRS by adding rCBF measurements and derived $rCMRO_2$, but its utility for anesthetic-depth monitoring requires prospective validation.

Declarations

Ethics approval and consent to participate

All animal procedures were approved by the Institutional Animal Care and Use Committee of the Gwangju Institute of Science and Technology (approval no. GIST-2019-060) and were carried out in

accordance with the institution's animal care guidelines. This study did not involve human participants, human data, or human tissue.

Consent for publication

Not applicable.

Competing interests

The authors declare that they have no competing interests.

Additional files

Additional file 1 (DOCX). Supplementary methods, figures, and tables. The Supplementary Methods define each analysis period, specify the group-specific 1.0% analysis windows, describe the derivation of rCBF, StO_2, ΔOHb, ΔRHb, ΔTHb, and $rCMRO_2$, and provide the statistical procedures. Figure S1 shows each animal's $rCMRO_2$ values across the protocol. Figure S2 aligns the AA rCBF and StO_2 traces around each animal's StO_2 peak. Figure S3 overlays the selected awake, maintenance, 1.0%, and recovery windows on the raw traces for every animal. Tables S1–S4 report within-group trends, values at each analyzed stage, paired comparisons between consecutive plotted analysis epochs, and sensitivity to awake-baseline window length. Tables S5 and S6 report the per-animal induction rCBF values and emergence latencies, respectively. Table S7 lists the anesthetic protocol and optical acquisition/model parameters. Table S8 compares the induction peak and maximum rate of increase for rCBF, StO_2, OHb, RHb, and THb, each normalized to its separate pre-induction awake value.

Additional file 2 (comma-separated values [CSV]). Source data for Figs. 2, 4, 5, and S1, including per-animal values of all six hemodynamic and metabolic measures at each analyzed stage.

Additional file 3 (CSV). Source data for Fig. 6 (per-animal behavioral emergence latencies).

Funding

This work was supported by the National Research Foundation of Korea (NRF) funded by the Ministry of Science, ICT & Future Planning (SGER grant NRF-2015R1D1A1A02062382; Brain Research Program NRF-2016M3C7A1905475); the InnoCORE program of the Ministry of Science and ICT (26-InnoCORE-01); the GIST Research Institute (GRI-GK0549A, 2016); the Biomedical Integrated Technology Research Project (GIST, 2016); the Research Development Fund of Xi'an Jiaotong-Liverpool University (RDF-23-01-119); and the Medical-Engineering Interdisciplinary Research Grant, Ruijin–XJTLU Intelligent Medicine Institute (2026JC024).

Author Contribution

Y.O. designed the study, developed the measurement system, performed the experiments, carried out the data analysis and statistics, and wrote the original draft. M.S. contributed to the methodology and system development, validated the results, and reviewed and edited the manuscript. S.C.K. and S.H.K. contributed to the methodology and instrumentation. J.B. provided the anesthesia protocol and medical advice. J.G.K. and J.Y.H. supervised the work and acquired funding. All authors read and approved the final manuscript.

Acknowledgements

Not applicable.

Availability of data and materials

The datasets generated and/or analyzed during the current study are available from the corresponding authors on reasonable request. The source data used to generate Figs. 2, 4, 5, 6, and S1 are provided as Additional files 2 and 3.

References

1. McKinstry-Wu AR, Wasilczuk AZ, Harrison BA, Bedell VM, Sridharan MJ, Breig JJ, et al. Analysis of stochastic fluctuations in responsiveness is a critical step toward personalized anesthesia. eLife. 2019;8:e50143. 10.7554/eLife.50143.
2. Brown EN, Lydic R, Schiff ND. General anesthesia, sleep, and coma. N Engl J Med. 2010;363(27):2638–50. 10.1056/NEJMra0808281.
3. Orser BA, Mazer CD, Baker AJ. Awareness during anesthesia. CMAJ. 2008;178(2):185–8. 10.1503/cmaj.071761.
4. Patel PM, Drummond JC. Cerebral physiology and the effects of anesthetic drugs. In: Miller RD, editor. Miller's Anesthesia. 7th ed. Philadelphia: Churchill Livingstone; 2010. pp. 305–39. 10.1016/B978-0-443-06959-8.00013-3.
5. Lee JG, Hudetz AG, Smith JJ, Hillard CJ, Bosnjak ZJ, Kampine JP. The effects of halothane and isoflurane on cerebrocortical microcirculation and autoregulation as assessed by laser-Doppler flowmetry. Anesth Analg. 1994;79(1):58–65. 10.1213/00000539-199407000-00012.
6. Slupe AM, Kirsch JR. Effects of anesthesia on cerebral blood flow, metabolism, and neuroprotection. J Cereb Blood Flow Metab. 2018;38(12):2192–208. 10.1177/0271678X18789273.
7. Drummond JC, Todd MM, Scheller MS, Shapiro HM. A comparison of the direct cerebral vasodilating potencies of halothane and isoflurane in the New Zealand white rabbit. Anesthesiology. 1986;65(5):462–7. 10.1097/00000542-198611000-00002.

8. Sebel PS, Lang E, Rampil IJ, White PF, Cork R, Jopling M, et al. A multicenter study of bispectral electroencephalogram analysis for monitoring anesthetic effect. Anesth Analg. 1997;84(4):891–9. 10.1097/00000539-199704000-00035.
9. Avidan MS, Zhang L, Burnside BA, Finkel KJ, Searleman AC, Selvidge JA, et al. Anesthesia awareness and the bispectral index. N Engl J Med. 2008;358(11):1097–108. 10.1056/NEJMoa0707361.
10. Rampil IJ. A primer for EEG signal processing in anesthesia. Anesthesiology. 1998;89(4):980–1002. 10.1097/00000542-199810000-00023.
11. Liang Z, Wang Y, Sun X, Li D, Voss LJ, Sleigh JW, et al. EEG entropy measures in anesthesia. Front Comput Neurosci. 2015;9:16. 10.3389/fncom.2015.00016.
12. Choi DH, Shin TJ, Kim S, Bae J, Cho D, Ham J, et al. Monitoring of cerebral oxygenation and local field potential with a variation of isoflurane concentration in a rat model. Biomed Opt Express. 2016;7(10):4114–24. 10.1364/BOE.7.004114.
13. Carp SA, Robinson MB, Franceschini MA. Diffuse correlation spectroscopy: current status and future outlook. Neurophotonics. 2023;10(1):013509. 10.1117/1.NPh.10.1.013509.
14. Boas DA, Yodh AG. Spatially varying dynamical properties of turbid media probed with diffusing temporal light correlation. J Opt Soc Am A. 1997;14(1):192–215. 10.1364/JOSAA.14.000192.
15. Durduran T, Yu G, Burnett MG, Detre JA, Greenberg JH, Wang J, et al. Diffuse optical measurement of blood flow, blood oxygenation, and metabolism in a human brain during sensorimotor cortex activation. Opt Lett. 2004;29(15):1766–8. 10.1364/OL.29.001766.
16. Culver JP, Durduran T, Furuya D, Cheung C, Greenberg JH, Yodh AG. Diffuse optical tomography of cerebral blood flow, oxygenation, and metabolism in rat during focal ischemia. J Cereb Blood Flow Metab. 2003;23(8):911–24. 10.1097/01.WCB.0000076703.71231.BB.
17. Roche-Labarbe N, Carp SA, Surova A, Patel M, Boas DA, Grant PE, et al. Noninvasive optical measures of CBV, StO_2, CBF index, and $rCMRO_2$ in human premature neonates' brains in the first six weeks of life. Hum Brain Mapp. 2010;31(3):341–52. 10.1002/hbm.20868.
18. Mesquita RC, Durduran T, Yu G, Buckley EM, Kim MN, Zhou C, et al. Direct measurement of tissue blood flow and metabolism with diffuse optics. Philos Trans Math Phys Eng Sci. 2011;369(1955):4390–406. 10.1098/rsta.2011.0232.
19. Tagliabue S, Lindner C, Chochron da Prat I, Sanchez-Guerrero A, Serra I, Kacprzak M, et al. Comparison of cerebral metabolic rate of oxygen, blood flow, and bispectral index under general anesthesia. Neurophotonics. 2023;10(1):015006. 10.1117/1.NPh.10.1.015006.
20. Cao R, Li J, Ning B, Sun N, Wang T, Zuo Z, et al. Functional and oxygen-metabolic photoacoustic microscopy of the awake mouse brain. NeuroImage. 2017;150:77–87. 10.1016/j.neuroimage.2017.01.049.
21. Samaei S, Shoemaker L, Kamar F, Milej D, Drosdowech D, Murkin JM, et al. Cerebral hemodynamic and metabolic responses to anesthesia and vasopressors in adult shoulder surgery: a 2×2 factorial

design randomized controlled trial with light-based neuromonitoring (CHEM-FACT study). Anesthesiology. 2026. 10.1097/ALN.0000000000006239.

22. Muzur A, Pace-Schott EF, Hobson JA. The prefrontal cortex in sleep. Trends Cogn Sci. 2002;6(11):475–81. 10.1016/s1364-6613(02)01992-7.
23. Libedinsky C, Livingstone M. Role of prefrontal cortex in conscious visual perception. J Neurosci. 2011;31(1):64–9. 10.1523/JNEUROSCI.3620-10.2011.
24. Farrell TJ, Patterson MS, Wilson B. A diffusion theory model of spatially resolved, steady-state diffuse reflectance for the noninvasive determination of tissue optical properties in vivo. Med Phys. 1992;19(4):879–88. 10.1118/1.596777.
25. Groenhuis RAJ, Ferwerda HA, Ten Bosch JJ. Scattering and absorption of turbid materials determined from reflection measurements. 1: Theory. Appl Opt. 1983;22(16):2456–62. 10.1364/AO.22.002456.
26. Verkruysse W, Lucassen GW, de Boer JF, Smithies DJ, Nelson JS, van Gemert MJ. Modelling light distributions of homogeneous versus discrete absorbers in light irradiated turbid media. Phys Med Biol. 1997;42(1):51–65. 10.1088/0031-9155/42/1/003.
27. Prahl S. Tabulated molar extinction coefficient for hemoglobin in water. Oregon Medical Laser Center; 1998. Available from: https://omlc.org/spectra/hemoglobin/summary.html. Accessed 6 Aug 2026.
28. Jacques SL. Optical properties of biological tissues: a review. Phys Med Biol. 2013;58(11):R37–61. 10.1088/0031-9155/58/11/R37.
29. Nachabé R, Evers D, Hendriks BHW, Lucassen GW, van der Voort M, Wesseling J, et al. Effect of bile absorption coefficients on the estimation of liver tissue optical properties and related implications in discriminating healthy and tumorous samples. Biomed Opt Express. 2011;2(3):600–14. 10.1364/BOE.2.000600.
30. Kim S, Kim M, Kim JG. Development of simple diffuse optical metabolic spectroscopy for tissue metabolism measurement. Biomed Opt Express. 2019;10(6):2956–66. 10.1364/BOE.10.002956.
31. Carp SA, Dai GP, Boas DA, Franceschini MA, Kim YR. Validation of diffuse correlation spectroscopy measurements of rodent cerebral blood flow with simultaneous arterial spin labeling MRI; towards MRI-optical continuous cerebral metabolic monitoring. Biomed Opt Express. 2010;1(2):553–65. 10.1364/BOE.1.000553.
32. Buckley EM, Hance D, Pawlowski T, Lynch JM, Wilson FB, Mesquita RC, et al. Validation of diffuse correlation spectroscopic measurement of cerebral blood flow using phase-encoded velocity mapping magnetic resonance imaging. J Biomed Opt. 2012;17(3):037007. 10.1117/1.JBO.17.3.037007.
33. Lemieux PA, Durian DJ. Investigating non-Gaussian scattering processes by using nth-order intensity correlation functions. J Opt Soc Am A. 1999;16(7):1651–64. 10.1364/JOSAA.16.001651.
34. Seong M, Oh Y, Lee K, Kim JG. Blood flow estimation via numerical integration of temporal autocorrelation function in diffuse correlation spectroscopy. Comput Methods Programs Biomed.

2022;222:106933. 10.1016/j.cmpb.2022.106933.

35. Diop M, Verdecchia K, Lee TY, St Lawrence K. Calibration of diffuse correlation spectroscopy with a time-resolved near-infrared technique to yield absolute cerebral blood flow measurements. Biomed Opt Express. 2011;2(7):2068–81. 10.1364/BOE.2.002068.
36. Verdecchia K, Diop M, Lee TY, St Lawrence K. Quantifying the cerebral metabolic rate of oxygen by combining diffuse correlation spectroscopy and time-resolved near-infrared spectroscopy. J Biomed Opt. 2013;18(2):027007. 10.1117/1.JBO.18.2.027007.
37. Lu H, Li Y, Li H, Yuan L, Liu Q, Sun Y, et al. Single-trial estimation of the cerebral metabolic rate of oxygen with imaging photoplethysmography and laser speckle contrast imaging. Opt Lett. 2015;40(7):1193–6. 10.1364/OL.40.001193.
38. Mann HB, Whitney DR. On a test of whether one of two random variables is stochastically larger than the other. Ann Math Stat. 1947;18(1):50–60. 10.1214/aoms/1177730491.
39. Hedges LV. Distribution theory for Glass's estimator of effect size and related estimators. J Educ Stat. 1981;6(2):107–28. 10.3102/10769986006002107.
40. Page EB. Ordered hypotheses for multiple treatments: a significance test for linear ranks. J Am Stat Assoc. 1963;58(301):216–30. 10.1080/01621459.1963.10500843.
41. Friedman M. The use of ranks to avoid the assumption of normality implicit in the analysis of variance. J Am Stat Assoc. 1937;32(200):675–701. 10.1080/01621459.1937.10503522.
42. Franceschini MA, Radhakrishnan H, Thakur K, Wu W, Ruvinskaya S, Carp S, et al. The effect of different anesthetics on neurovascular coupling. NeuroImage. 2010;51(4):1367–77. 10.1016/j.neuroimage.2010.03.060.
43. Masamoto K, Fukuda M, Vazquez A, Kim SG. Dose-dependent effect of isoflurane on neurovascular coupling in rat cerebral cortex. Eur J Neurosci. 2009;30(2):242–50. 10.1111/j.1460-9568.2009.06812.x.
44. Huppert TJ, Jones PB, Devor A, Dunn AK, Teng IC, Dale AM, et al. Sensitivity of neural-hemodynamic coupling to alterations in cerebral blood flow during hypercapnia. J Biomed Opt. 2009;14(4):044038. 10.1117/1.3210779.
45. Masamoto K, Kanno I. Anesthesia and the quantitative evaluation of neurovascular coupling. J Cereb Blood Flow Metab. 2012;32(7):1233–47. 10.1038/jcbfm.2012.50.
46. Hoffman WE, Edelman G, Kochs E, Werner C, Segil L, Albrecht RF. Cerebral autoregulation in awake versus isoflurane-anesthetized rats. Anesth Analg. 1991;73(6):753–7. 10.1213/00000539-199112000-00013.
47. Eintrei C, Leszniewski W, Carlsson C. Local application of 133Xenon for measurement of regional cerebral blood flow (rCBF) during halothane, enflurane, and isoflurane anesthesia in humans. Anesthesiology. 1985;63(4):391–4. 10.1097/00000542-198510000-00008.
48. Cucchiara RF, Theye RA, Michenfelder JD. The effects of isoflurane on canine cerebral metabolism and blood flow. Anesthesiology. 1974;40(6):571–4. 10.1097/00000542-197406000-00011.

49. Gelman S, Fowler KC, Smith LR. Regional blood flow during isoflurane and halothane anesthesia. Anesth Analg. 1984;63(6):557–65. 10.1213/00000539-198406000-00002.
50. Flynn NM, Buljubasic N, Bosnjak ZJ, Kampine JP. Isoflurane produces endothelium-independent relaxation in canine middle cerebral arteries. Anesthesiology. 1992;76(3):461–7. 10.1097/00000542-199203000-00021.
51. Farber NE, Harkin CP, Niedfeldt J, Hudetz AG, Kampine JP, Schmeling WT. Region-specific and agent-specific dilation of intracerebral microvessels by volatile anesthetics in rat brain slices. Anesthesiology. 1997;87(5):1191–8. 10.1097/00000542-199711000-00024.
52. Matta BF, Heath KJ, Tipping K, Summors AC. Direct cerebral vasodilatory effects of sevoflurane and isoflurane. Anesthesiology. 1999;91(3):677–80. 10.1097/00000542-199909000-00019.
53. Todd MM, Drummond JC. A comparison of the cerebrovascular and metabolic effects of halothane and isoflurane in the cat. Anesthesiology. 1984;60(4):276–82. 10.1097/00000542-198404000-00002.
54. Maekawa T, Tommasino C, Shapiro HM, Keifer-Goodman J, Kohlenberger RW. Local cerebral blood flow and glucose utilization during isoflurane anesthesia in the rat. Anesthesiology. 1986;65(2):144–51. 10.1097/00000542-198608000-00003.
55. Hansen TD, Warner DS, Todd MM, Vust LJ. The role of cerebral metabolism in determining the local cerebral blood flow effects of volatile anesthetics: evidence for persistent flow-metabolism coupling. J Cereb Blood Flow Metab. 1989;9(3):323–8. 10.1038/jcbfm.1989.50.
56. Hyder F, Rothman DL, Shulman RG. Total neuroenergetics support localized brain activity: implications for the interpretation of fMRI. Proc Natl Acad Sci USA. 2002;99(16):10771–6. 10.1073/pnas.132272299.
57. Cohen ER, Ugurbil K, Kim SG. Effect of basal conditions on the magnitude and dynamics of the blood oxygenation level-dependent fMRI response. J Cereb Blood Flow Metab. 2002;22(9):1042–53. 10.1097/00004647-200209000-00002.
58. Alkire MT, Haier RJ, Barker SJ, Shah NK, Wu JC, Kao YJ. Cerebral metabolism during propofol anesthesia in humans studied with positron emission tomography. Anesthesiology. 1995;82(2):393–403. 10.1097/00000542-199502000-00010.
59. Berndt N, Kovács R, Schoknecht K, Rösner J, Reiffurth C, Maechler M, et al. Low neuronal metabolism during isoflurane-induced burst suppression is related to synaptic inhibition while neurovascular coupling and mitochondrial function remain intact. J Cereb Blood Flow Metab. 2021;41(10):2640–55. 10.1177/0271678X211010353.
60. Wasilczuk AZ, Harrison BA, Kwasniewska P, Ku B, Kelz MB, McKinstry-Wu AR, et al. Resistance to state transitions in responsiveness is differentially modulated by different volatile anaesthetics in male mice. Br J Anaesth. 2020;125(3):308–20. 10.1016/j.bja.2020.05.031.
61. Friedman EB, Sun Y, Moore JT, Hung HT, Meng QC, Perera P, et al. A conserved behavioral state barrier impedes transitions between anesthetic-induced unconsciousness and wakefulness: evidence for neural inertia. PLoS ONE. 2010;5(7):e11903. 10.1371/journal.pone.0011903.

62. Wasilczuk AZ, Meng QC, McKinstry-Wu AR. Electroencephalographic evidence for individual neural inertia in mice that decreases with time. Front Syst Neurosci. 2022;15:787612. 10.3389/fnsys.2021.787612.

Figures

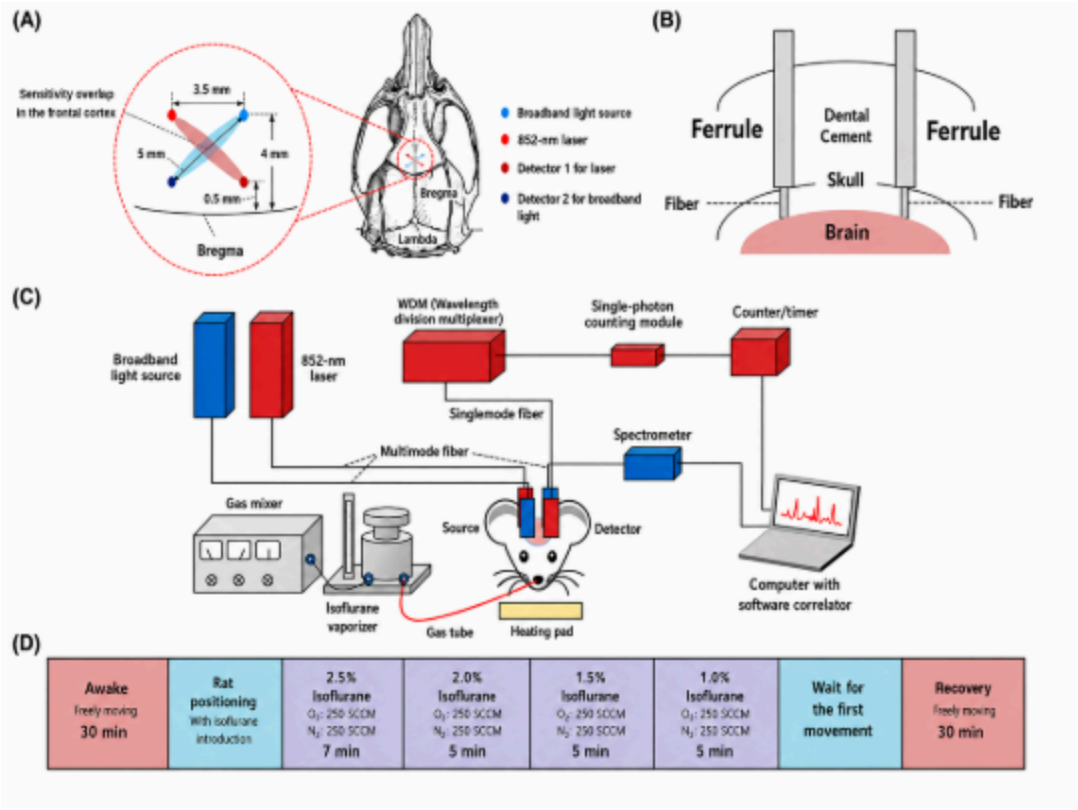


Figure 1

Experimental design and optical setup. (A) Optode geometry on the rat skull (dorsal view, referenced to bregma/lambda): the four ferrules were placed bilaterally at 0.5 and 4.0 mm anterior to bregma and 1.75 mm lateral to the midline. The diagonal source–detector separation for each modality was approximately 5 mm, and the bilateral optodes within each anterior–posterior row were 3.5 mm apart. (B) Sagittal schematic of the implanted ferrules and fibers fixed to the skull with dental cement, coupling light into and out of the cortex. (C) Instrumentation: an 852-nm diffuse correlation spectroscopy (DCS) source and a broadband diffuse reflectance spectroscopy (DRS) source delivered light through separate fibers to the frontal cortex. Light collected by the DCS detector fiber passed through the wavelength division multiplexer (WDM) to the single-photon counting module and counter/timer, whereas diffusely reflected light collected by the DRS detector fiber was sent to the spectrometer. Breathing gas mixed with isoflurane was delivered via a gas tube connected to a vaporizer/gas mixer, and body temperature was maintained with a heating pad. (D) Protocol timeline: 30-min awake baseline, anesthesia induction with 3.0% isoflurane in 50% oxygen and positioning, four stepwise maintenance stages (2.5, 2.0, 1.5, and 1.0% isofluranein 50% oxygen; 2.5% isoflurane for 7 min, subsequent stages 5 min each), isoflurane

discontinuation followed by observation until the first spontaneous movement, and a 30-min recovery recording.

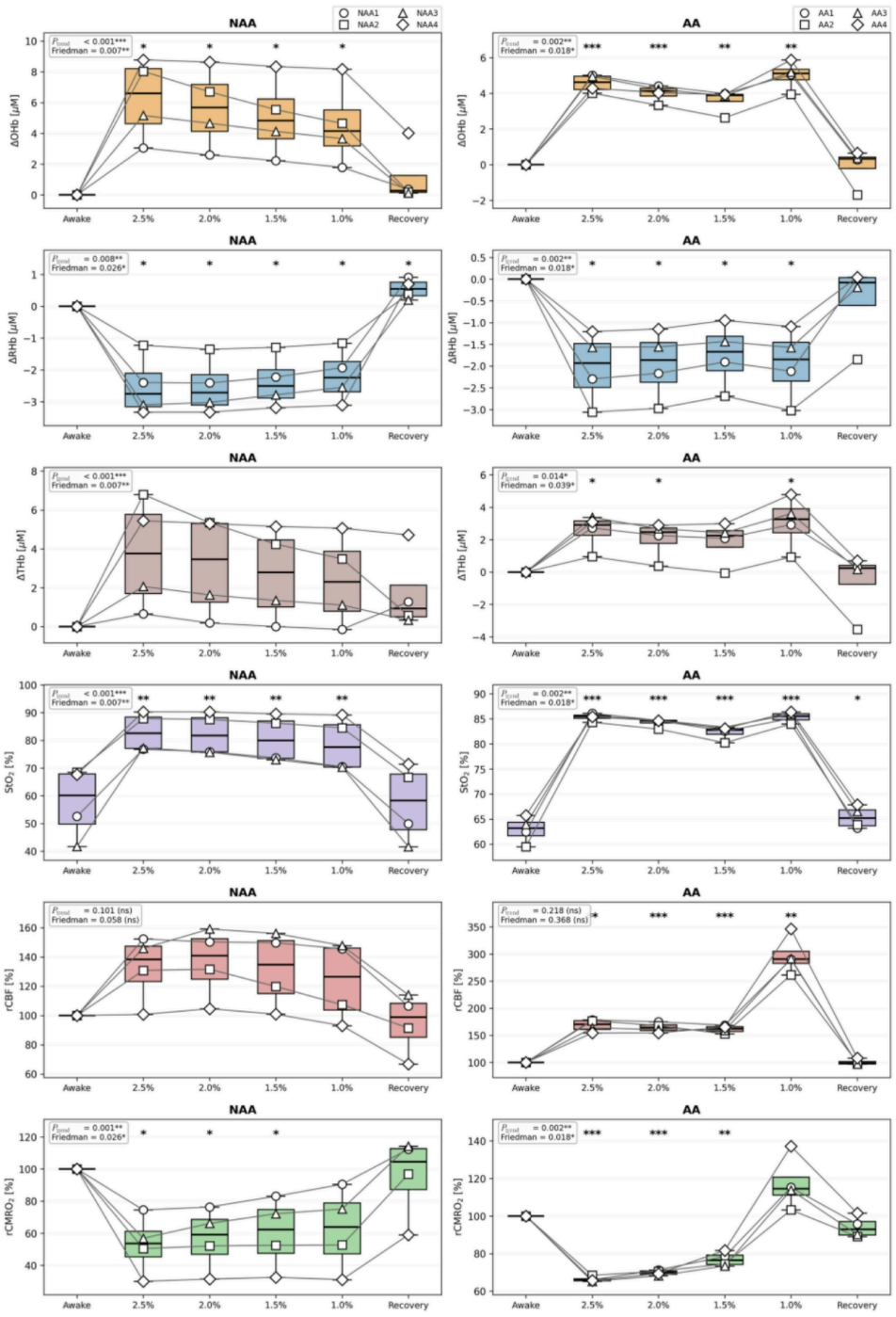


Figure 2

Relative cerebral blood flow (rCBF), tissue oxygen saturation (StO_2), concentration changes from the awake baseline in oxygenated hemoglobin (ΔOHb), deoxygenated hemoglobin (ΔRHb), and total

hemoglobin (ΔTHb), and derived relative cerebral metabolic rate of oxygen ($rCMRO_2$) during the awake baseline, isoflurane maintenance, and recovery periods in 'not awake during anesthesia' (NAA) and 'awake during anesthesia' (AA) animals. The left and right columns show the NAA and AA groups, respectively. Box plots show the awake baseline, four maintenance concentrations (2.5, 2.0, 1.5, and 1.0% isoflurane), and recovery, with per-animal values connected across periods. Awake and recovery values were calculated over 120-s windows. Maintenance values were calculated from the final 60 s of each stage, except for the AA values at 1.0%, which were calculated over 60-s windows centered on each animal's StO_2 peak. The Page and Friedman tests included all four maintenance concentrations in NAA animals and the 2.5, 2.0, and 1.5% concentrations in AA animals. The plotted AA values at 1.0% were excluded from the Page and Friedman tests. P_{trend}, Page's trend-test p; Friedman, Friedman-test p; ns, not significant. *: $p < 0.05$, **: $p < 0.01$, and ***: $p < 0.001$ for two-sided paired t-tests against the awake baseline ($n = 4$ per group). Source data are provided in Additional file 2.

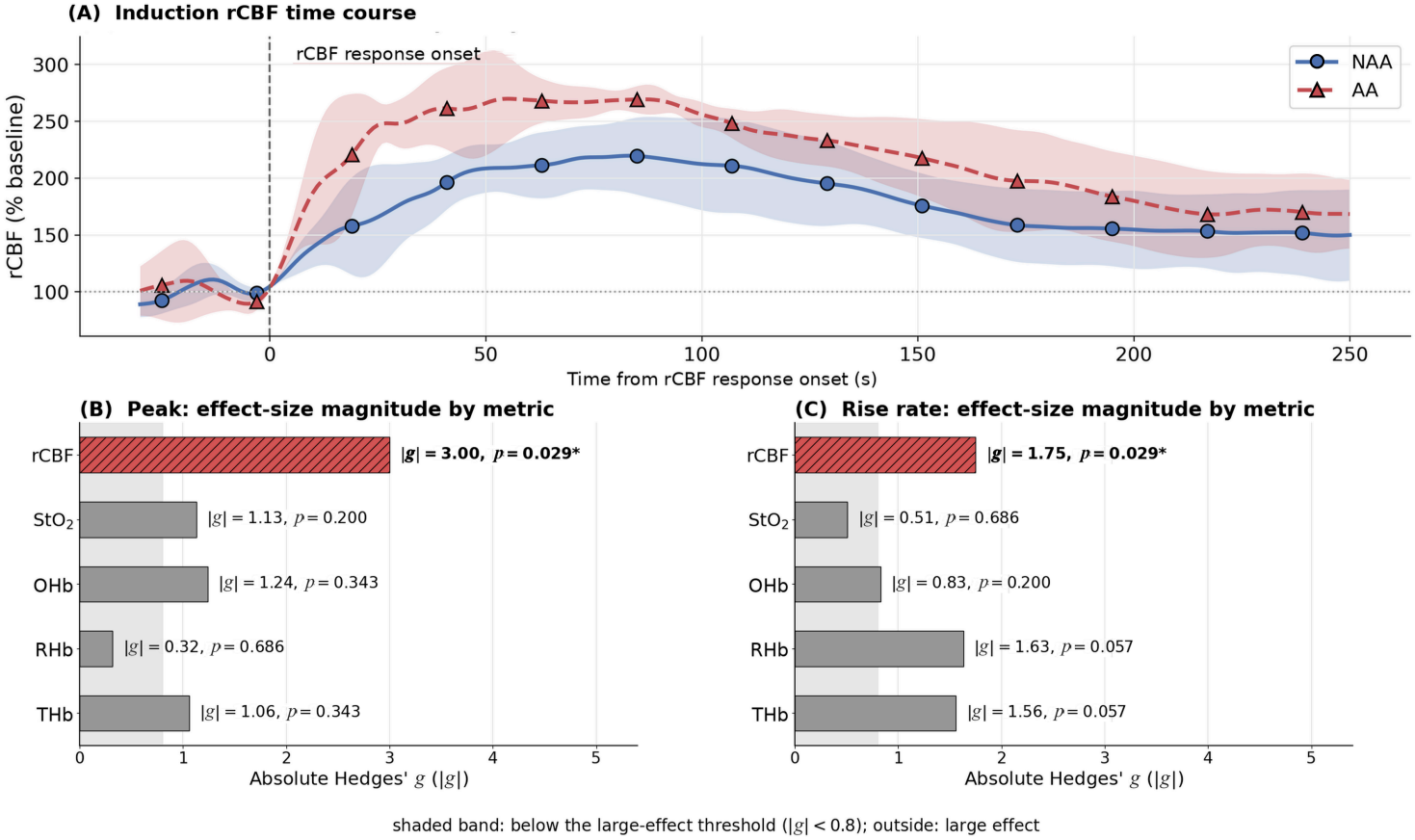


Figure 3

Induction rCBF time course and between-group effect sizes. (A) Group-mean rCBF aligned to the rCBF response onset (mean ± standard deviation (SD)). (B) Absolute Hedges' g ($|g|$) for the difference between AA and NAA animals in the induction peak of rCBF, StO_2, OHb, RHb, and THb. (C) $|g|$ for the difference between AA and NAA animals in the maximum rate of increase of rCBF, StO_2, OHb, RHb, and THb. For the induction analysis, each measure was expressed as a percentage of its own separate pre-induction awake value, defined as 100%. The plotted $|g|$ values show the magnitude, but not the direction, of each

AA–NAA difference. Additional file 1: Table S8 reports the means of AA and NAA and the *p*-values for every comparison. Only rCBF differed significantly between groups for the induction peak (|*g*| = 3.00, *p* = 0.029) and for the maximum rate of increase (|*g*| = 1.75, *p* = 0.029). These *p*-values were obtained with two-sided exact Mann–Whitney U tests. Based on the unrounded group means, peak rCBF was 38% higher in AA than in NAA, and the maximum rate of rCBF increase in AA was 94% higher than in NAA. The shaded band marks |*g*| values below the conventional large-effect threshold of 0.8. Per-animal rCBF values are provided in Additional file 1: Table S5. Peak and maximum-rate values were calculated for each animal before group means, effect sizes, and *p*-values were obtained.

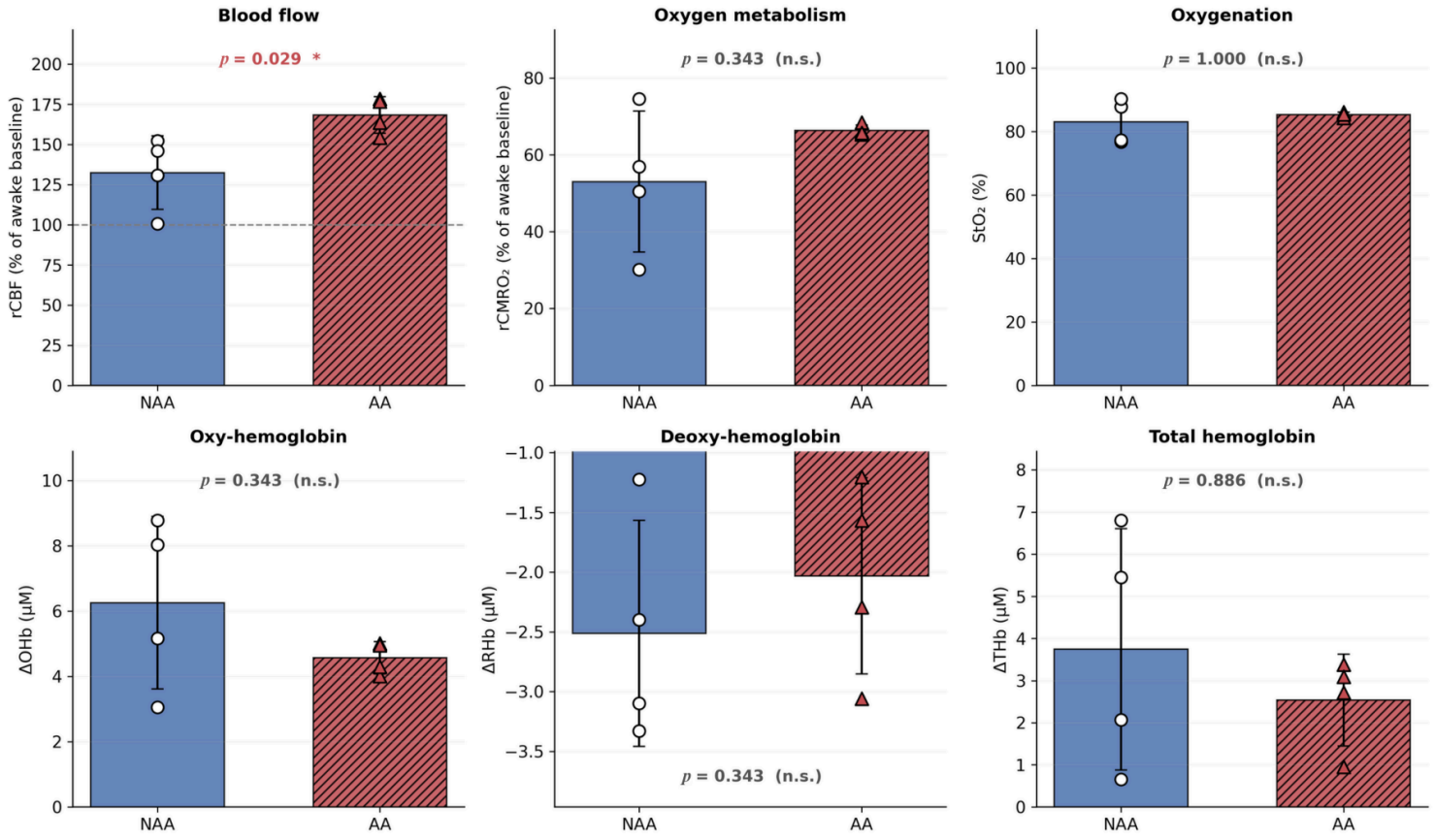


Figure 4

Between-group comparison of the six hemodynamic and metabolic measures at 2.5% isoflurane. Group mean ± SD, and per-animal values (NAA: white circle; AA: red triangle) are shown. Mean rCBF was significantly higher in AA than in NAA animals (*p* = 0.029). $rCMRO_2$ (*p* = 0.343), ΔOHb (*p* = 0.343), ΔRHb (*p* = 0.343), ΔTHb (*p* = 0.886), and StO_2 (*p* = 1.0) did not differ significantly between groups. *n*.s., not significant.

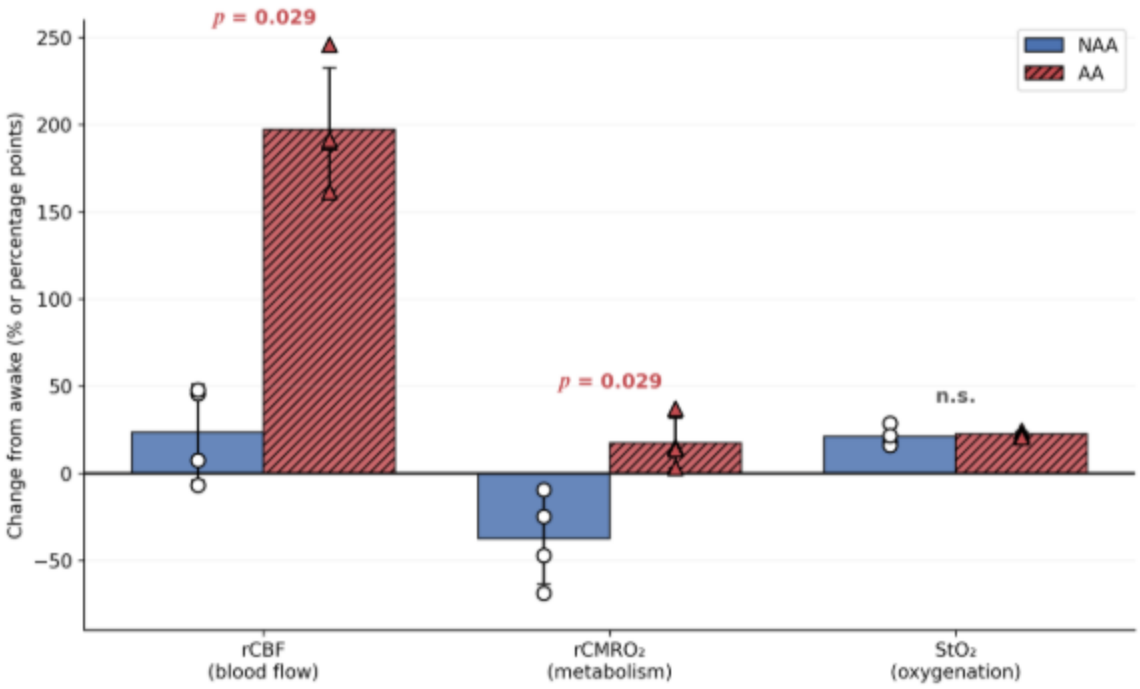


Figure 5

Changes from the awake baseline at 1.0% isoflurane, using a 60-s StO_2-peak-centered window for AA animals and the final 60 s of the stage for NAA animals. Bars show group means ± SD. For rCBF and $rCMRO_2$, relative change was calculated as [(value during the group-specific 1.0% analysis window / awake-baseline value) − 1] × 100%. The StO_2 change was calculated by subtracting the awake-baseline saturation from the saturation during the 1.0% analysis window and is reported as percentage points. In AA animals, mean rCBF was 197% above the awake baseline (297% of the baseline value), and mean $rCMRO_2$ was 17% above the awake baseline. In NAA animals, mean $rCMRO_2$ was 38% below the awake baseline. The rCBF change was significantly greater in AA than in NAA animals (Mann–Whitney U test $p = 0.029$). The $rCMRO_2$ change was also significantly greater in AA than in NAA animals ($p = 0.029$). The StO_2 change did not differ significantly between groups (+22.5 percentage points in AA and +21.0 percentage points in NAA; $p = 0.486$). Per-animal $rCMRO_2$ values are shown in Additional file 1: Fig. S1.

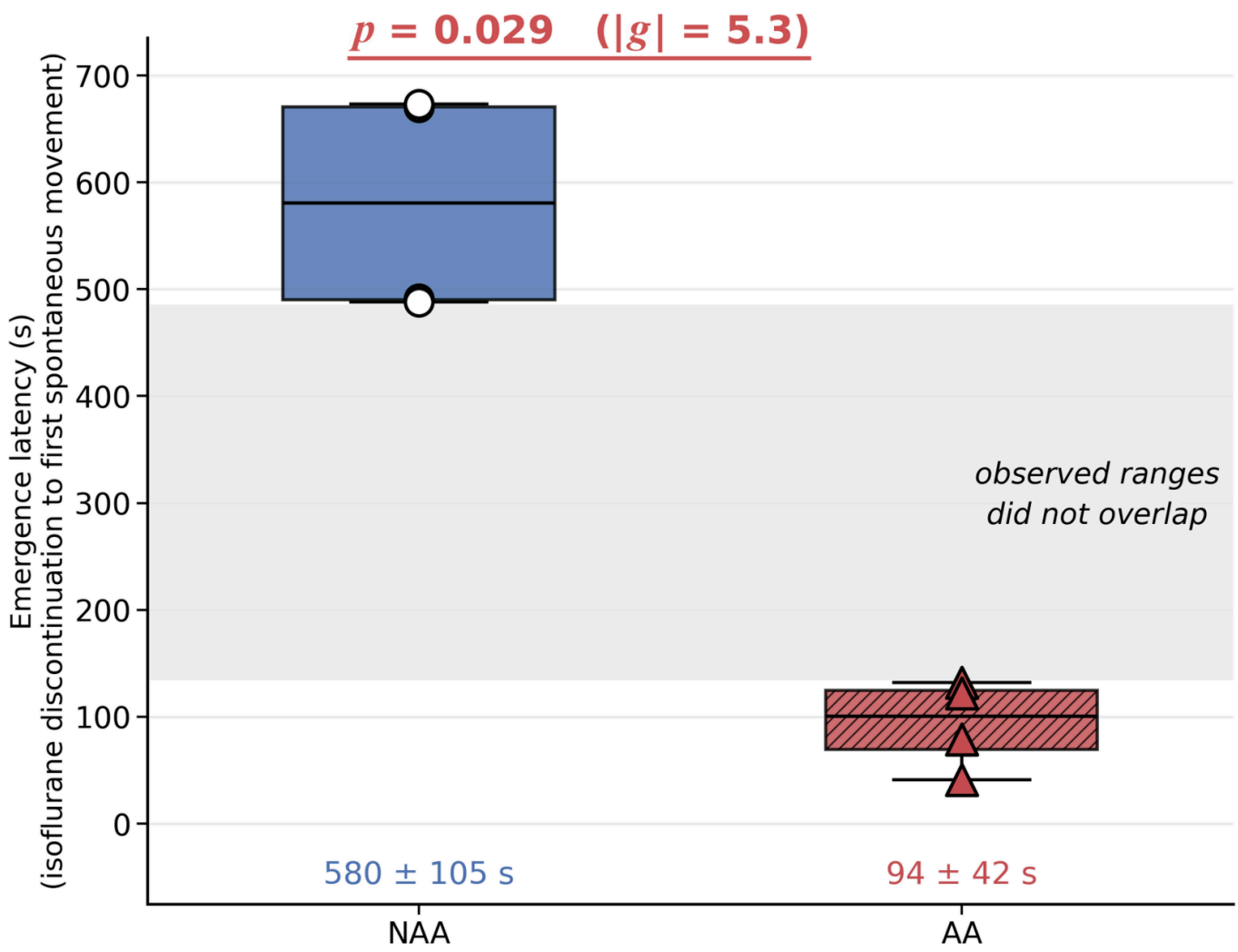


Figure 6

Time from isoflurane discontinuation to the first observed spontaneous movement in AA and NAA animals. Per-animal values and group box plots are shown (n = 4 per group). Mean emergence latency was 94 ± 42 s in AA animals and 580 ± 105 s in NAA animals (Mann–Whitney U test p = 0.029, $|g|$ = 5.3). The shaded region marks the interval between the longest AA latency and the shortest NAA latency. Latency was measured by real-time behavioral observation. Source data are provided in Additional file 3.

Supplementary Files

This is a list of supplementary files associated with this preprint. Click to download.

- 3Table1.docx
- 4Additionalfile1.docx